Study of the Transformations of Elemental Nanowires to Nanotubes of Metal Oxides and Chalcogenides through the Kirkendall Effect

Kalyan Raidongia and C. N. R. Rao*

Chemistry and Physics of Materials Unit, Jawaharlal Nehru Centre for Advanced Scientific Research, Jakkur P.O., Bangalore, 560064, India

Received: May 17, 2008; Revised Manuscript Received: July 1, 2008

We have employed the Kirkendall effect to transform elemental nanowires of metals and silicon to nanotubes of the corresponding oxides and chalcogenides, having prepared the metal nanowires by nebulized spray pyrolysis of metal acetates in an inert atmosphere and silicon nanowires by carbon-assisted synthesis. The formation of ZnO nanotubes by the oxidation of Zn nanowires has been studied as a function of time observing the intermediate structures during the oxidation. Nucleation of Kirkendall voids in the nanowires during the oxidation leads to the formation of the ZnO nanotubes. The kinetics of the Zn nanowire−ZnO nanotube transformation has been studied and the activation energy for the transformation found to be 12.2 kcal/mol, a value smaller than that for bulk metal oxidation. $ZnCr_2O_4$ nanotubes are formed by the reaction of Zn nanowires with CrO_2Cl_2 in an oxygen atmosphere. We have obtained nanotubes of Co_3O_4, starting from Co nanowires and SiO_2 (cristobalite) nanotubes starting from Si nanowires. Nanotubes of ZnS, CdS, and CdSe have been obtained by the reaction of the metal nanowires with the chalcogens. The activation energy for the formation of CdS nanotubes from Cd nanowires is found to be only 8.5 kcal/mol. The present study establishes the Kirkendall effect as a novel means of preparing nanotube structures of several inorganic materials.

Introduction

Nanotubes are nanomaterials of great importance due to their novel properties and potential applications in diverse areas as high-efficiency catalysts, drug delivery systems, nanoelectronics, nano-optics, lightweight structural materials and energy storage and conversion.[1,2] Compared to nanowires, nanotubes provide access to three different contact regions: the inner surface, the outer surface and the tube ends. Several methods of synthesizing carbon as well as inorganic nanotubes have been described in the literature.[1,2] Typical of the synthetic methods are template-assisted growth, arc discharge, laser ablation, chemical vapor deposition, plasma enhanced vaporization and hydrothermal or solvothermal processes. Hollow nanostructures can also be created by making use of the Kirkendall effect. Synthesis of nanotube-like hollow nanostructures employing the Kirkendall effect would have several advantages.[3] The Kirkendall effect involves a nonequilibrium mutual diffusion process of a diffusion couple through the interface such a directional flow of atoms is balanced by the flow of vacancies.[4] When the nanostructure of a fast-diffusing species reacts with a slower-diffusing species, a large number of vacancies are created because of the high surface to volume ratio of the nanostructure as well as the absence of defects at the core. Inside the small volume of the growing nanostructure the vacancies coalesce into large voids giving rise to products which are hollow nanostructures. Hollow spherical nanostructures of cobalt oxides, sulfides and selenides have been obtained by making use of the Kirkendall effect.[5] Nanotubes of Ag_2Se have been prepared by UV photodissociation of CSe_2 adsorbed on the surface of Ag nanowires.[6] While Ga doped ZnS nanowires have been converted in to ZnO-$ZnGa_2O_4$ composite nanotubes.[7] $ZnAl_2O_4$ nanotubes are obtained by the interfacial solid state reaction of core−shell ZnO−Al_2O_3 nanowires.[8] Formation of Co_3S_4 nanotubes starting from 1D $Co(CO_3)_{0.35}Cl_{0.20}(OH)_{1.10}$ nanowires appears to involve the Kirkendall effect.[9] In spite of these literature reports, there is no detailed investigation of the structures as well as the formation kinetics of 1D hollow nanostructure of oxides and other materials formed by the transformations of metallic or elemental nanowires through the Kirkendall effect. We have, therefore, carried out a systematic study of the formation of nanotubes of a variety of materials from the elemental nanowires. Thus, formation of ZnO nanotubes from Zn nanowires has been investigated by employing X-ray diffraction and electron microscopy, paying attention to the process of transformation. $ZnCr_2O_4$ nanotubes have been formed by the reaction of Zn nanowires with CrO_2Cl_2. We have obtained nanotubes of Co_3O_4, ZnS, CdS and CdSe starting with the corresponding metallic nanowires, besides SiO_2 (cristobalite) nanotubes starting from Si nanowires. Kinetics of formation of the CdS nanotubes from Cd nanowires has also been examined. The choice of the elemental nanowires used in the study was based on the ease of oxidation and other reactions involved and the variety of elements examined was to establish the versatility of the process.

Experimental Section

Nanowires of Zn, Co, and Cd were synthesized by the nebulized spray pyrolysis of methanolic solutions of the metal acetates in an inert atmosphere.[10] In a typical experiment, a 50 mL methanolic solution of acetate of zinc, cadmium or cobalt was prepared with a concentration of 40 g L^{-1}. The solution was nebulized and the spray carried into a preheated silicon carbide furnace maintained between 1093 and 1123 K using Ar as a carrier gas. Typical flow rates of Ar used was 1000 standared cubic centimeter per minute (sccm). All the experiments were performed using a quartz tube with an inner diameter

* Corresponding author. E-mail: cnrrao@jncasr.ac.in. Fax: +91.80. 22082760.

10.1021/jp8043658 CCC: $40.75
Published on Web 08/12/2008

of 25 mm. The reaction was typically carried out for 1 h. The shiny deposits obtained at the outlet of quartz tube was characterized to be metal nanowires and used for the further experiments.

Si nanowires were obtained by heating an intimate mixture of silicon powder and activated charcoal in nitrogen environment.[11] In typical experiment silicon powder was finely ground with activated charcoal keeping the weight ratio of Si to C at 1:3 and the mixture was heated at 1473 K for 3 h in an N_2 atmosphere. The gray color powder obtained as final product was characterized to be Si nanowires and used for further experiments.

The Zn nanowires were heated at around 703 K for 4 h in air to transform them to ZnO nanotubes. The progress of the reaction was followed by recording electron microscopy images as well as X-ray diffraction patterns at intermediate stages of the transformation. The kinetic data were obtained by recording X-ray diffraction patterns at different stages of the conversion in the 653−703 K range. We have carried out the reaction of Zn nanowires with CrO_2Cl_2 at 673 K for 3 h to obtain $ZnCr_2O_4$ nanotubes. CrO_2Cl_2 was produced in a gas trap by adding a mixture of KCl and $K_2Cr_2O_7$ to concentrated H_2SO_4. In a typical experiment, a mixture of 1 g KCl and 1 g $K_2Cr_2O_7$ was added to 25 mL of conc H_2SO_4. Oxygen gas was passed through the trap to carry the CrO_2Cl_2 vapor toward the Zn nanowires placed in a tube furnace. In order to prepare Co_3O_4 nanotubes, Co nanowires were heated in air at 773 K for 5 h. The intermediate structures during Co_3O_4 nanotubes formation was examined at 723 K/5 h. To prepare SiO_2 nanotubes, oxidation of Si nanowires was carried out at 1598 K for 5 h in air.

Zn nanowires (30 mg) were mixed thoroughly with sulfur powder (150 mg) and the mixture was heated in an Ar atmosphere at 773 K for 3 h to obtain ZnS nanotubes. CdS nanotubes were synthesized by heating a finely ground mixture of Cd nanowires and sulfur powder (1:9 molar ratio) at 773 K for 3 h in an Ar atmosphere. The kinetics of the reaction was studied by recording XRD patterns at different time intervals. CdSe nanotubes were obtained by heating a mixture of Cd nanowires and selenium powder (1:5 molar ratio) at 673 K for 3 h in an Ar atmosphere.

X-ray diffraction (XRD) patterns were recorded at 298 K with a Rich-Siefert 3000-TT diffractometer employing Cu Kα radiation. Field emission scanning electron microscopy (FESEM) and scanning tunnelling electron microscopy (STEM) images were recorded with a field emission scanning electron microscope (FESEM, FEI Nova-Nano SEM-600, Netherlands). TEM images were recorded with a JEOL JEM 3010 instrument (Japan) operated at an accelerating voltage of 300 kV.

Results and Discussion

In Figure 1a, we show a low-magnification FESEM image of Zn nanowires obtained by nebulized spray pyrolysis of a methanolic solution of zinc acetate. The nanowires have lengths of several tens of micrometers with zigzag morphology. The higher magnification FESEM image in Figure 1b, shows the nanowires to have a smooth surface with an average diameter 50 nm. The TEM image in Figure 1c, along with the selected area electron diffraction (SAED) pattern shown as an inset, confirms the nanowires to be single crystalline. The X-ray diffraction (XRD) pattern (Figure 1d) is characteristic of the hexagonal structure of zinc (JCPDS card: No. 04−0831, a = 2.67 Å and b = 4.95 Å).

Thermal oxidation of Zn nanowires in air in the temperature range 653−703 K for 2−4 h was found to yield ZnO nanotubes.

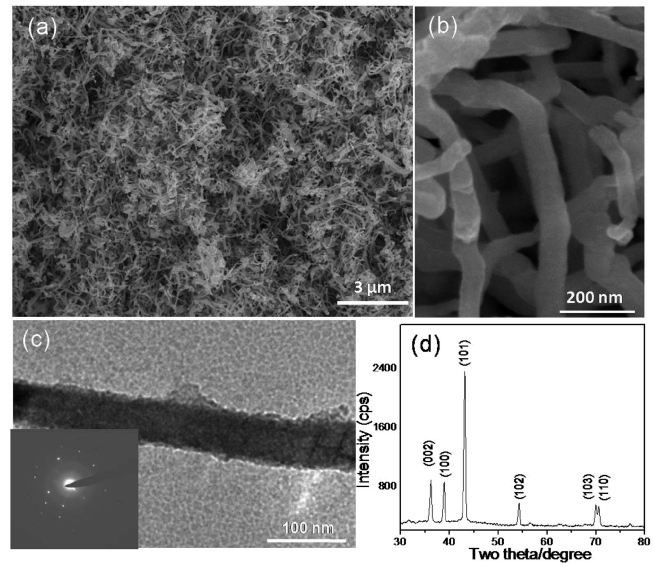

Figure 1. (a) Low-magnification and (b) higher-magnification FESEM images of Zn nanowires, (c) TEM image of a Zn nanowire (the inset is the SAED pattern), and (d) XRD pattern of Zn nanowires.

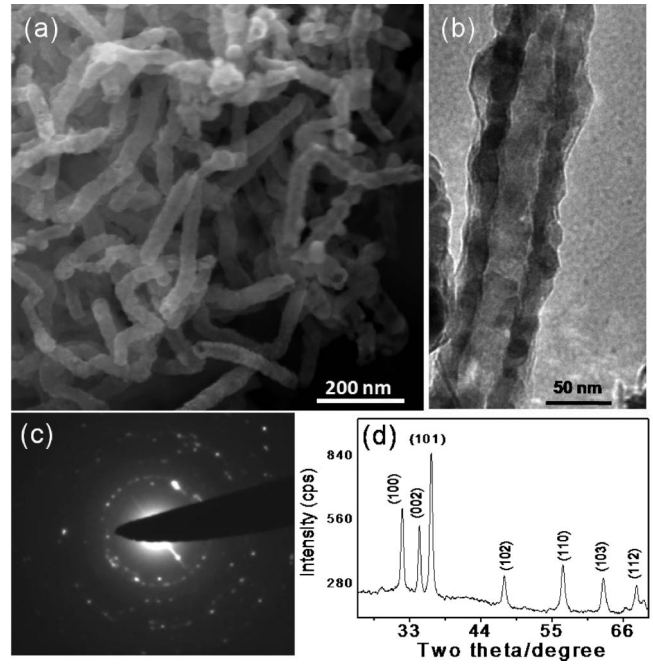

Figure 2. (a) FESEM image of ZnO nanotubes, (b) TEM image of a ZnO nanotube, (c) SAED pattern of ZnO nanotube, and (d) XRD pattern of ZnO nanotubes.

The tubular structure of ZnO nanotubes is clearly seen in the FESEM image (Figure 2a). There is a distribution in the diameters of the nanotubes just as in the diameters of the starting nanowires. The outer diameters of the nanotubes go up to 90 nm with lengths varying from 400 nm to few micrometers. The TEM image of a ZnO nanotube shown in Figure 2b demonstrates the wall thickness to be around 20 nm. Thus, the inner diameter of the nanotubes works out to be close to the diameter of the starting metal nanowires. The SAED pattern of the ZnO nanotube (Figure 2c) shows some ring patterns, but with prominent Bragg spots. The XRD pattern shown in Figure 2d could be indexed on the hexagonal unit cell of ZnO (JCPDS card: No. 36-14151, $P6_3mc$, a = 5.25 Å and c = 5.21 Å).

The formation of ZnO nanotubes by the oxidation of Zn nanowires was studied as a function of time, observing the

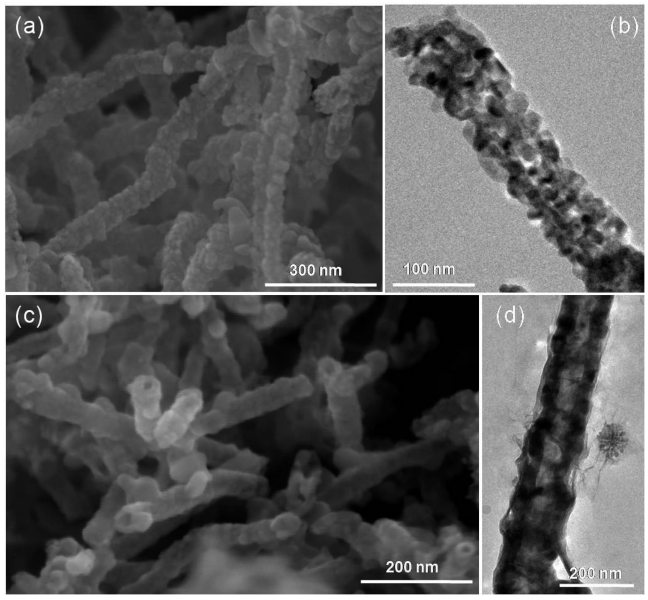

Figure 3. (a) FESEM image and (b) TEM image of the nanostructure obtained after oxidation for 15 min, (c) FESEM image, and (d) TEM image obtained after 1 h of oxidation.

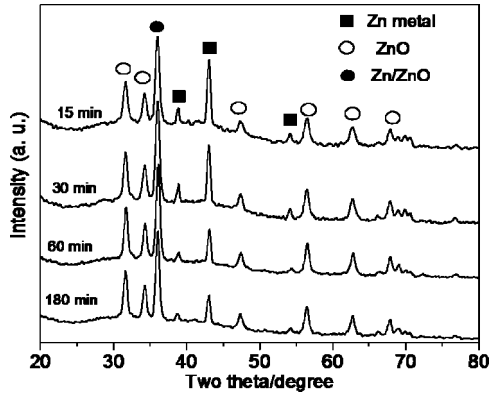

Figure 4. XRD patterns recorded at different time intervals of the Zn nanowires-ZnO nanotubes transformation.

intermediate structures during the oxidation of the metal nanowires. A FESEM image of Zn nanowires after oxidation for 15 min is shown in Figure 3a. In this intermediate stage of oxidation, we see the rough surface of the 1D nanostructure compared to the initial smooth surface of Zn nanowires. A TEM image in Figure 3b reveals the porous nature of nanostructure. After oxidation for 1 h, the surface roughness of the nanostructure decreases and openings of tube-like structures begin to appear as can be seen from the FESEM image in Figure 3c. The pores formed after oxidation for 15 min coalesce to form bigger pores resulting a bamboo type nanotube structure after 1 h as shown in the TEM image in Figure 3d. After the oxidation was carried out for 4 h, well-defined nanotubes of ZnO are formed as shown in Figure 2. The porous nature of the intermediate nanostructures and the polycrystalline nature of the product nanotubes suggest that the conversion of Zn nanowires into ZnO nanotubes involves nanoscale Kirkendall effect.[5−9,12] The faster outer diffusion of zinc atoms compared to the slower inner diffusion of the oxygen atoms through the initially formed ZnO layer is compensated by the opposite flow of vacancies, the vacancies coalescing together to form larger Kirkendall voids. The Kirkendall voids condense into form the bigger holes in the nanostructures, giving rise to bamboo-like morphology. After this stage, it takes another 2−3 h to form

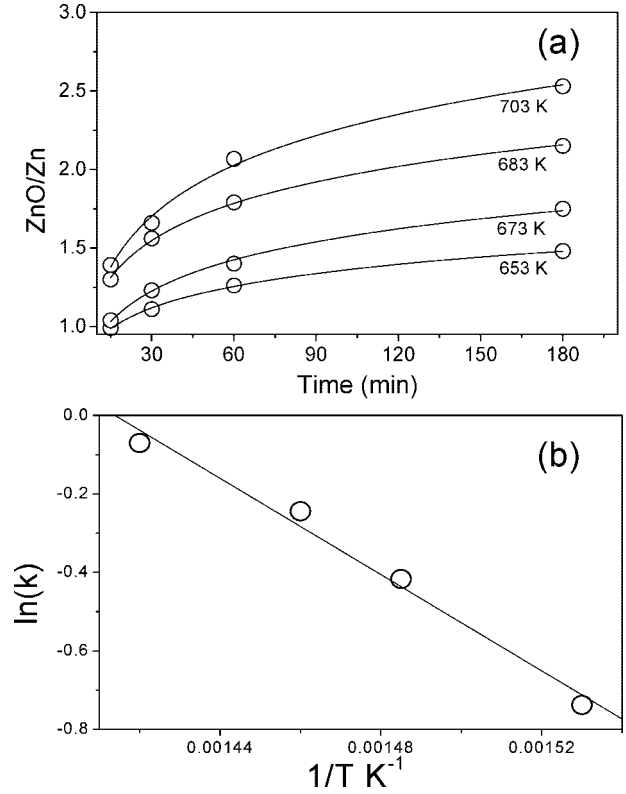

Figure 5. (a) Plots of the ratios of areas under ZnO (100) and Zn (101) reflections against reaction time at different temperatures (open symbols). Solid curves represent the logarithimic rate law fit to the experimental data. (b) Arrhenius plot of lnk against 1/T.

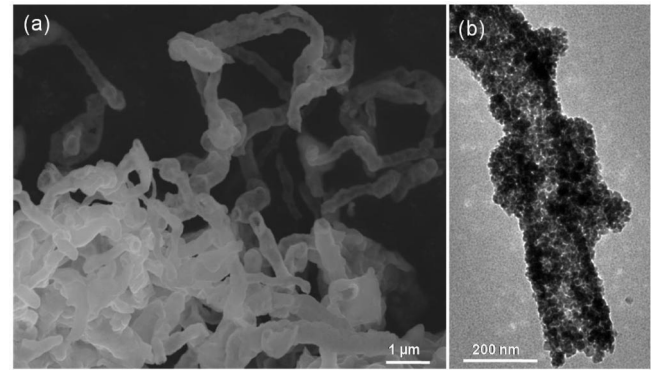

Figure 6. (a) FESEM image of $ZnCr_2O_4$ nanotubes, (b) TEM image of a $ZnCr_2O_4$ nanotube.

perfect tubular nanostructures since the increasing thickness of the ZnO layer does not favor the outer diffusion of Zn atoms.

The kinetics of formation ZnO nanotubes was studied by recording XRD patterns at different time intervals at 653, 673, 683, and 703 K. The reflections correspond to both Zn and ZnO coexist in all the patterns shown in Figure 4, but the reflections corresponding to ZnO increase in intensity with time, accompanied by a decrease in the intensity of the reflections due to Zn metal. We have determined the areas under the (100) reflection of ZnO and the (101) reflection of Zn and plotted the ZnO:Zn ratio of areas against the reaction time in Figure 5a (open symbols) at different temperatures. These experimental data could be fitted to the logarithimic rate law.

$$y = k \log(at + 1) + b \quad (1)$$

where t is time in minutes, k is the rate constant, a and b are temperature-dependent constants, and y is the ZnO/Zn ratio. The

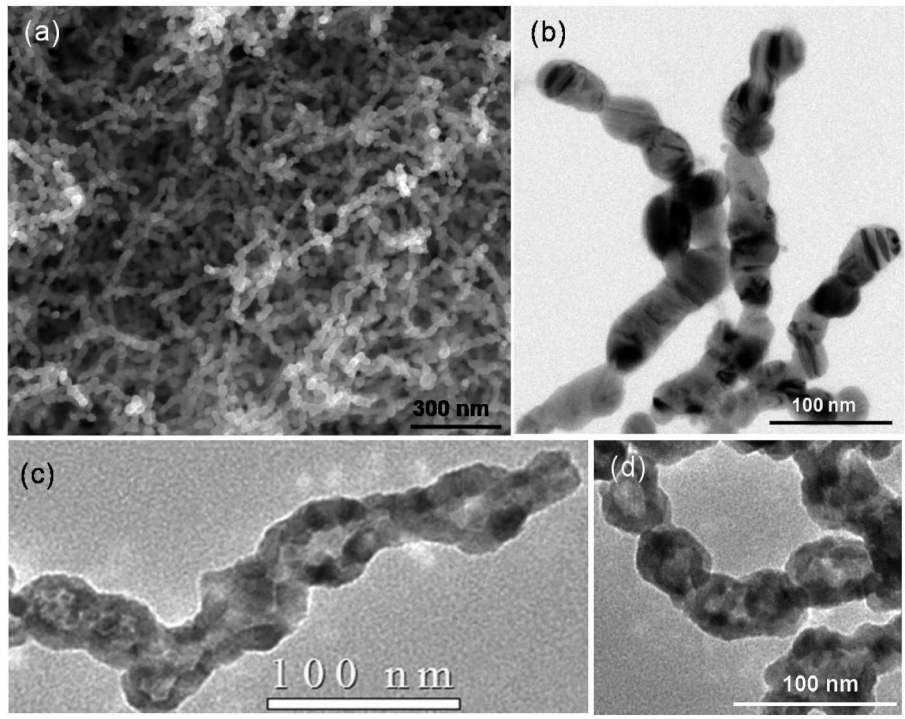

Figure 7. (a) FESEM image and (b) TEM image of Co nanowires, (c) TEM image of a Co_3O_4 nanotube, and (d) TEM image of the intermediate stage of a Co_3O_4 nanotube formation.

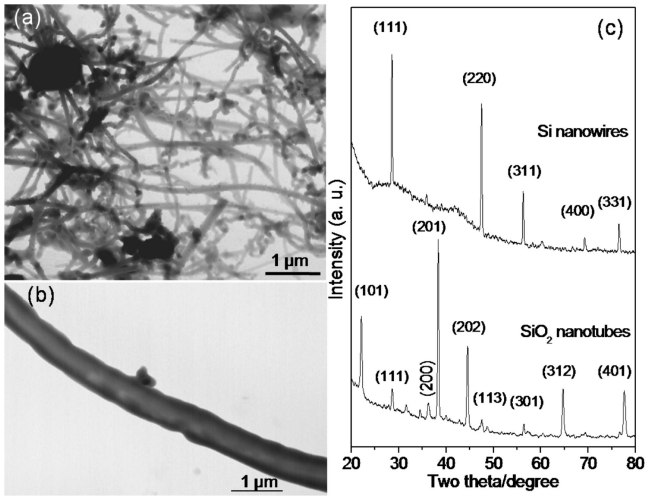

Figure 8. STEM images of (a) Si nanowires and (b) SiO_2 nanotube; (c) XRD patterns of Si nanowires and SiO_2 nanotubes.

logarithmic rate law is widely used to explain the oxidation of metals,[13−18] arises from the mechanism proposed by Caberra and Mott, Grimley and Trapwell, and Eley and Wilkinson, where either cation or anion diffusion limits the rate of oxide growth.[16−20] There is an initial period of rapid oxidation followed by a virtual cessation of the reaction and the formation of a stable film, a few nanometers in thickness. The goodness of the fits of the experimental data to eq 1 can be seen by the solid curves shown in Figure 5a. From these data, we have derived the value of k in eq 1. A plot of lnk against inverse of absolute temperature is given in Figure 5b. This plot yields an activation energy for the nanotubes formation of 12.2 kcal/mol. The activation energy for the oxidation of bulk Zn is repoted to be 28.1 kcal/mol.[21,22] Thus, the activation energy for the oxidation by the Kirkendall effect involving diffusion processes is associated with a lower activation energy. The lower activation energy is likely to be due to the larger surface area of the nanostructures and also due to the Kirkendall mechanism involved.

We have obtained nanotubes of $ZnCr_2O_4$ by the reaction of Zn nanowire with CrO_2Cl_2. A low magnification FESEM image of the $ZnCr_2O_4$ nanotubes is shown in Figure 6a. The nanotubes replicate the zigzag morphology of the starting Zn nanowires. The nanowires have lengths of several micrometers while the diameter varies between 150 and 500 nm. Open ends of the nanotubes are clearly seen in the FESEM image in Figure 6a. The TEM image of $ZnCr_2O_4$ nanotube in Figure 6b reveals the porous nature of nanotubes. The nanotubes have a granular wall, with a thickness of 20−30 nm. The SAED pattern shows rings, due to the polycrystalline nature of the $ZnCr_2O_4$ nanotubes. The XRD pattern of the nanotubes is characteristic of the cubic structure $ZnCr_2O_4$ (JCPDF card: No. 22-1107, $a = 8.32$ Å).

Figure 7a shows a FESEM image of Co nanowires with a necklaces-like structure obtained by the nebulized spray pyrolysis of a methanolic solution of Co acetate. The nanowires have a narrow diameter distribution (20−25 nm range) with lengths of several micrometers. The TEM image in Figure 7b reveals that the nanowires are formed by head to tail fusion of linearly arranged spindle-shaped nanoparticles. A TEM image of a Co_3O_4 nanotube obtained by the thermal oxidation of Co nanowires at 773 K in air is shown in Figure 7c. The outer diameter of the nanotube is around 40 nm, with a wall thickness of 10 nm. The inner diameter of the nanotube is similar to the diameter of starting Co nanowires indicating that the nanotube is formed by the dominant outer diffusion of cobalt atoms through the initially formed oxide layer on the surface of nanowires. As the starting nanowires have necklace-like morphology, the walls of the product nanotubes are not parallel and there are some humps at the fusion points. The intermediate stage of the Co_3O_4 nanotubes formation was examined by transmission electron microscopy. The TEM image in Figure 7d reveals that the Kirkendall holes localized inside the

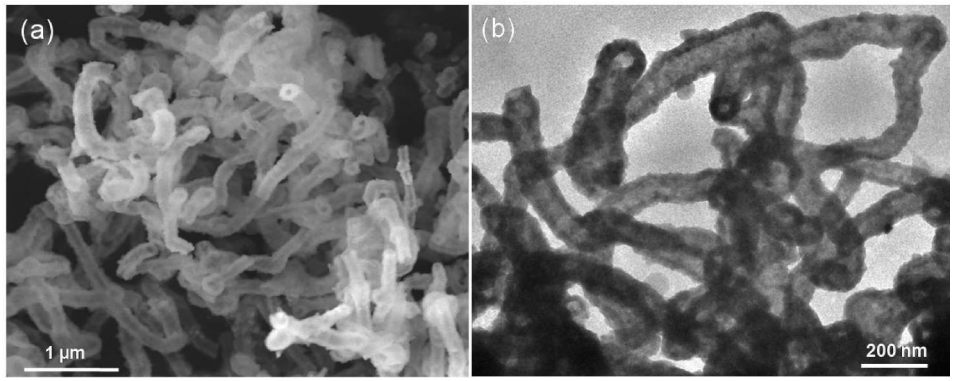

Figure 9. (a) FESEM image and (b) TEM image of ZnS nanotubes.

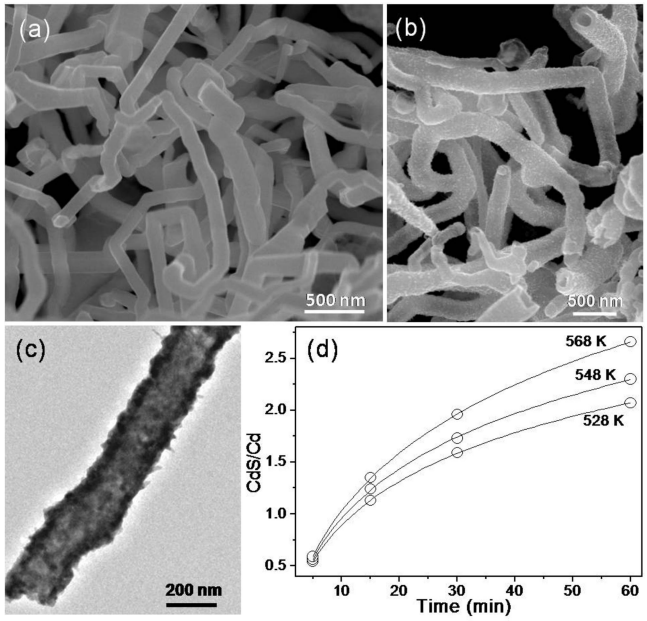

Figure 10. FESEM images of (a) Cd nanowires and (b) CdS nanotubes and the (c) TEM image of a CdS nanotube. (d) Plots of the ratios of areas under CdS (110) and Cd (101) reflections against reaction time at different temperatures (open symbols). Solid curves represent the logarithimic rate law fit to the experimental data.

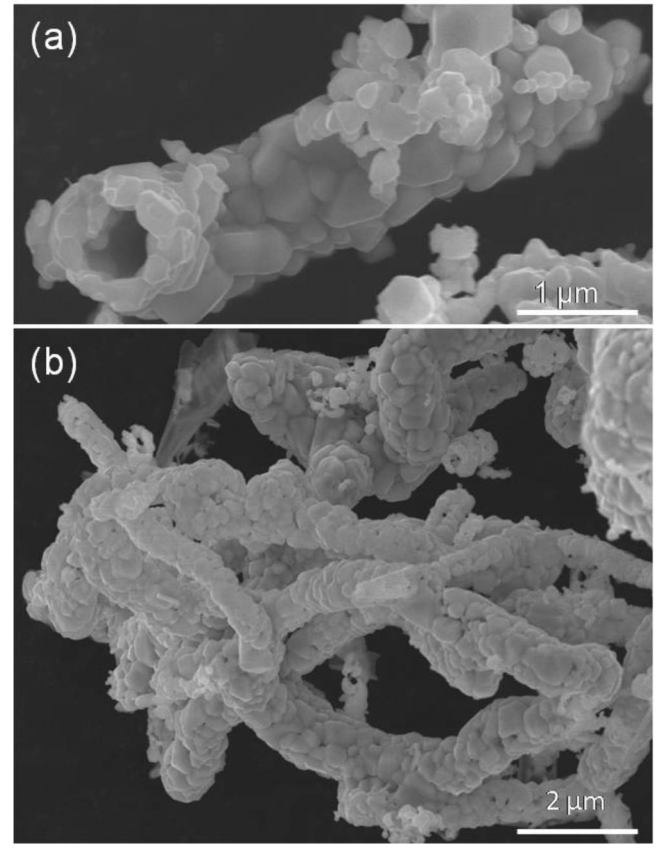

Figure 11. (a and b) FESEM images of CdSe nanotubes.

interconnected nanoparticles during intermediate stage of oxidation. When heated at higher temperature the localized holes get interconnected to form the continuous tubular structure.

In Figure 8a, we show a STEM image of Si nanowires obtained by heating an intimate mixture of silicon powder and activated charcoal in a nitrogen environment. The nanowires have diameters ranging from 100 to 400 nm and lengths of several tens micrometers. The XRD pattern of the nanowires shown in Figure 8c matches with that of cubic silicon (JCPDF card: No. 03-0544, $a = 5.42$ Å). Si nanowires were heated up to 1598 K to obtain nanotubes of SiO_2 shown in the STEM image in Figure 8b. The diameter of the nanotubes is around 700 nm with wall thickness of around 100 nm. Figure 8c shows the XRD pattern of the nanotubes, the strong intensity of the peaks indicates high crystallinity of the nanotubes. All the peaks could be indexed on the tetragonal SiO_2 structure of cristobalite with the lattice parameters, $a = 4.9$ Å and $c = 6.9$ Å (JCPDF card: No. 04-0379). The SiO_2 nanotubes obtained here are unusual in that they are crystalline, unlike most silica nanotubes which are amorphous.

Reaction of Zn nanowires with sulfur powder yields abundant quantities of ZnS nanotubes. The FESEM image in Figure 9a shows that the ZnS nanotubes have lengths of few micrometers with zigzag morphology similar to starting Zn nanowires. A low magnification TEM image of ZnS nanotubes is shown in Figure 9b. The outer diameter of the nanotubes is around 100 nm with wall thickness of 20−25 nm. The XRD pattern of the as prepared nanotubes reveals the formation of phase-pure ZnS with the cubic structure (JCPDF card: No. 01-0792, $a =$ 5.4 Å).

Cd nanowires prepared by nebulized spray pyrolysis (see the FESEM image in Figure 10a) had diameters varying from 80 to 400 nm, with lengths of several micrometers. The Cd nanowires have a smooth surface with zigzag morphology. The XRD pattern of the nanowires is characteristic of the hexagonal structure of cadmium (JCPDF card: No. 85-1328, $a = 2.97$ Å, $c = 5.61$ Å). Cadmium nanowires were transformed into CdS nanotubes by heating with sulfur powder in an Ar atmosphere at 773 K for 3 h. In Figure 10b, we show a FESEM image of the CdS nanotubes. The nanotubes have a smooth surface with

diameter in the range of 100 to 500 nm. The length of nanotubes goes up to several micrometers just as the starting Cd nanowires. A TEM image of individual CdS nanotube is shown in Figure 10c. The diameter of this nanotube is around 200 nm with a wall thickness of 30−40 nm. The XRD pattern of the CdS nanotubes establishes the hexagonal structure with lattice parameters of $a = 4.1$ Å and $c = 6.7$ Å (JCPDF card: No. 01-0783).

The kinetics of the transformation of the Cd nanowires to CdS nanotubes was studied by recording the XRD patterns after different periods of the reaction at 528, 548 and 568 K. These XRD patterns clearly show increase in the intensity of the CdS reflections with time. The ratios of areas under the (110) reflection of CdS and the (101) reflections of Cd are plotted against time in Figure 10d. The solid lines in Figure 10d show the fits of the experimental data to logarithimic rate law as given by eq 1. From the rate constants so obtained, we estimate the activation energy for the conversion to be 8.5 kcal/mol. The activation energy reported for the formation of an anodic film of CdS on a Cd electrode is 10.6 kcal/mol.[23] Formation of CdS nanocrystals starting from Cd−stearate and tributylphosphine sulfide in a paraffin hot matrix involves an activation energy of 51.9 kcal/mol.[24] Thus, the conversion of Cd nanowires to CdS nanotubes involves a lower activation energy than that for bulk conversions.

It has been possible to obtain CdSe nanotubes starting from Cd nanowires. In Figure 11a, we show a FESEM image of a single CdSe nanotube obtained by heating an intimate mixture Cd nanowires and Se powder. The nanotubes have a diameter of around 800 nm with a wall thickness in the range of 200 to 250 nm. The granular wall of the nanotube is made up of CdSe nanocrystals. A low magnification FESEM image of CdSe nanotubes is shown in Figure 11b. The XRD pattern of the nanotubes is showed to have the cubic structure. (JCPDF card: No. 03-0544, $a = 5.42$ Å).

Conclusions

We have investigated the structures as well as the formation kinetics of 1D hollow nanostructure of oxides and other materials formed by the transformation of elemental nanowires through Kirkendall effect. A detailed study of the formation of ZnO nanotubes starting from Zn nanowires has been carried out by employing X-ray diffraction and electron microscopy. The transformation requires only a small activation energy of 12.2 kcal/mol. Nanotubes of $ZnCr_2O_4$ are obtained by the reaction of Zn nanowires with CrO_2Cl_2 in oxygen. It has been possible to obtained nanotubes of SiO_2, Co_3O_4, ZnS, CdS and CdSe by the reaction of the corresponding elemental nanowires with oxygen or the chalcogen. In the case of SiO_2, the nanotubes are crystalline with the cristobalite structure. The activation energy of formation of CdS nanotubes is also small. The present study demonstrates how Kirkendall effect can be exploited as a novel means of producing nanotubes of a variety of inorganic materials. Furthermore, the study throws light on the mechanism of the Kirkendall effect in forming hollow nanotubes from nanowires.

References and Notes

(1) Rao, C. N. R.; Govindaraj, A. *Nanotubes and Nanowires*; RSC Publishing: Cambridge, U.K., 2005.
(2) Rao, C. N. R.; Vivekchand, S. R. C.; Biswas, K.; Govindaraj, A. *Dalton Trans.* **2007**, *34*, 3728.
(3) Fan, H. J.; Gosele, U.; Zacharias, M. *small* **2007**, *3*, 1660.
(4) Smigelskas, A. D.; Kirkendall, E. O. *Trans. AIME* **1947**, *171*, 130.
(5) Yin, Y.; Rioux, R. M.; Erdonmez, C. K.; Hughes, S.; Somorjai, G. A.; Alivisatos, A. P. *Science* **2004**, *304*, 711.
(6) Ng, C. H. B.; Tan, H.; Fan, W. Y. *Langmuir* **2006**, *22*, 9712.
(7) Gautam, U. K.; Bando, Y.; Zhan, J.; Costa, P. M. F. J.; Fang, Golberg, X. D. *Adv. Mater.* **2008**, *20*, 810.
(8) Fan, H. J.; Knez, M.; Scholz, R.; Nielsch, K.; Pippel, E.; Hesse, D.; Zacharias, M.; Gosele, U. *Nat. Mater.* **2006**, *5*, 627.
(9) Chen, X.; Zhang, Z.; Qiu, Z.; Shi, C.; Li, X. *J. Colloid Interface Sci.* **2007**, *308*, 271.
(10) Vivekchand, S. R. C.; Gundiah, G.; Govindaraj, A.; Rao, C. N. R. *Adv. Mater.* **2004**, *16*, 1842.
(11) Gundiah, G.; Deepak, F. L.; Govindaraj, A.; Rao, C. N. R. *Chem. Phys. Lett.* **2003**, *381*, 579.
(12) Kim, D.; Park, J.; An, K.; Yang, N. K.; Park, J. G.; Hyeon, T. *J. Am. Chem. Soc.* **2007**, *129*, 5812.
(13) Nwoko, V. O.; Uhlig, H. H. *J. Electrochem. Soc.* **1965**, *112*, 1181.
(14) Vernon, W. H. J.; Calnan, E. A.; Clews, C. J. B.; Nurse, T. *J. Proc. R. Soc. London, A* **1953**, *216*, 375.
(15) Konetzki, R. A.; Chang, Y. A. *J. Mater. Res.* **1989**, *4*, 1421.
(16) Mott, N. F. *Trans. Faraday Soc.* **1947**, *43*, 429.
(17) Formhold, A. T. J. *J. Phys. Chem. Solids* **1963**, *24*, 1081.
(18) Young, D. J.; Dignam, M. J. *Oxid. Met.* **1972**, *5*, 241.
(19) Maschhoff, B. L.; Armstrong, N. R. *Langmuir* **1991**, *7*, 693.
(20) Cobrera, N.; Mott, N. F. *Rep. Prog. Phys.* **1949**, *12*, 163.
(21) Moore, W. J.; Lee, J. K. *Trans. Faraday Soc.* **1951**, *45*, 501.
(22) Moore, W. J. *J. Chem. Phys.* **1952**, *20*, 764.
(23) Yeh, L-S. R.; Hudson, P. G.; Damjanovic, A. *J. Appl. Electrochem.* **1982**, *12*, 153.
(24) Yordanov, G. G.; Adachi, E.; Dushkin, C. D. *Colloids Surf. A.* **2006**, *289*, 118.

JP8043658